

Electrochemical Study of Doxorubicin Interaction with Different Sequences of Double Stranded Oligonucleotides, Part II

David Hynek^{1,2}, Ludmila Krejcová^{1,2}, Ondrej Zitka^{1,2}, Vojtech Adam^{1,2}, Libuse Trnkova^{2,3,4}, Jiri Sochor^{1,2}, Marie Stiborova⁵, Tomas Eckschlager⁶, Jaromir Hubalek^{1,2,7} and Rene Kizek^{1,2,7,*}

¹ Department of Chemistry and Biochemistry, Faculty of Agronomy, Mendel University in Brno, Zemedelska 1, CZ-613 00 Brno, Czech Republic, European Union

² Central European Institute of Technology, Brno University of Technology, Technicka 3058/10, CZ-616 00 Brno, Czech Republic, European Union

³ Department of Chemistry, and ⁴ Research Centre for Environmental Chemistry and Ecotoxicology, Faculty of Science, Masaryk University, Kotlarska 2, CZ-611 37 Brno, Czech Republic, European Union

⁵ Department of Biochemistry, Faculty of Science, Charles University, Albertov 2030, CZ-128 40 Prague 2, Czech Republic, European Union

⁶ Department of Paediatric Haematology and Oncology, 2nd Faculty of Medicine, Charles University, V Uvalu 84, CZ-150 06 Prague 5, Czech Republic, European Union

⁷ Department of Microelectronics, Faculty of Electrical Engineering and Communication, Brno University of Technology, Technicka 3058/10, CZ-616 00 Brno, Czech Republic, European Union

*E-mail: kizek@sci.muni.cz

Received: 15 June 2011 / Accepted: 26 October 2011 / Published: 1 January 2012

Interaction of low molecular weight compounds with DNA is one of general mechanisms utilized for an effective anticancer therapy. The anthracycline doxorubicin is one of the drugs that represent the compound with such effect. In our previous work [Hynek et al., Int. J. Electrochem. Sci. 7 (2012) xx] the electrochemical behaviour of doxorubicin interaction with single stranded ODN by using adsorptive transfer stripping square wave voltammetry was described. This paper is focused on the study of interaction of doxorubicin with double stranded ODNs (dsODNs) using the same technique. Here, we used four dsODNs possessing different primary structures and observed the changes in their electrochemical behaviour after their treatment with three concentrations of doxorubicin for 5 hours. The changes found are discussed and differences in behaviours of individual dsODNs described and associated with their structure.

Keywords: intercalating drug; doxorubicin; hetero-nucleotides; square wave voltammetry; adsorptive transfer stripping technique; adriamycin; DNA

1. INTRODUCTION

Deoxyribonucleic acid (DNA) belongs among the most extensively studied biomolecules. Currently, much attention has been devoted to the study of variety compounds interacting with DNA, which can be used for cancer treatment. Anthracycline antibiotic doxorubicin, also called adriamycin, belongs to the substances interacting with DNA used for the above mentioned purposes [1,2]. It is commonly used in the treatment of many cancers [3]. The following mechanisms were considered: 1) intercalation into DNA, leading to inhibited DNA replication and transcription; 2) generation of free radicals, leading to DNA damage or lipid peroxidation; 3) DNA binding and alkylation; 4) DNA cross-linking; 5) interference with DNA unwinding or DNA strand separation and helicase activity; 6) direct membrane effects; and 7) inhibition of topoisomerase II [2,3]. In spite of these suggestions the exact mechanism of action this drug on a tumour has not been precisely elucidated, however, there is a great research in the field to improve effectiveness and reduce its toxicity [4,5]. For these purposes nanotechnology and nano-based materials and their combination with electrochemistry [6] are often discussed, because drug targeting via nanoparticles as carriers is a promising way of cancer treatment, which avoids the side effects of conventional chemotherapy.

1.1 Nanomedicine application

1.1.1 *In vivo* analysis and imaging

Several studies dealt with the interaction of nanoparticles with doxorubicin. The effect of Cd²⁺-enriched CdS nanoparticles on the electrochemical behaviour and hydrophobic/hydrophilic properties of doxorubicin-DNA target system was investigated by using *in situ* electrochemical contact angle measurements. It was observed that those nanoparticles could remarkably affect the contact angle variation between oxidation and reduction forms of doxorubicin upon application of the corresponding potentials. Moreover, the site-selective DNA binding of doxorubicin in the presence of CdS nanoparticles was demonstrated by both electrochemical contact angle measurements and atomic force microscopy studies, indicating that CdS nanoparticles could facilitate the interaction of doxorubicin with DNA and accordingly influence the hydrophobic/hydrophilic properties of the target system during the biological recognition process. These observations suggest that the nano-interface of CdS may offer great promising application in biomolecular recognition [7-9]. Moreover, magnetic multi-walled nanotubes (MWNT) combined with near-infrared radiation-assisted desorption was successfully developed for the determination of tissue distribution of doxorubicin liposome injects in rats. The magnetic MWNT nanomaterials were synthesized via a simple hydrothermal process. Magnetic Fe₃O₄ beads, with average diameters of about 200 nm and narrow size distribution, were decorated along MWNTs to form octopus-like nanostructures. The hybrid nanocomposites provided an efficient way for the extraction and enrichment of doxorubicin onto the polyaromatic surface of MWNTs. Doxorubicin adsorbed with magnetic MWNTs could be simply and rapidly isolated through a magnetic field. In addition, due to the near-infrared radiation absorption property of MWNTs, irradiation with NIR laser was employed to induce photothermal conversion, which could trigger rapid

doxorubicin desorption from DOX-loaded magnetic MWNTs [10]. It was also reported the interaction of doxorubicin covalently bound via tether molecules to colloidal magnetic nanoparticles (ferrofluid) with calf thymus double stranded DNA (dsDNA). Using spectroscopic and electrochemical techniques, the authors demonstrated that appropriate length and flexibility of tether molecules allows the preservation of essentially intact intercalation capabilities of free doxorubicin in the solution. In order to evaluate these capabilities, they studied the binding constant of doxorubicin attached to nanoferrites with dsDNA as well as the binding site size on the dsDNA molecule. The binding constant decreased slightly compared to that of free doxorubicin while the binding site size, describing the number of consecutive DNA lattice residues involved in the binding, increased. Atomic force microscopy (AFM) and scanning electron microscopy (SEM) images were also employed to support the conclusion on the interactions between doxorubicin-modified magnetic nanoparticles and dsDNA [11]. Zhang et al. and Zhou et al. showed that tetraheptylammonium capped magnetic nano Fe_3O_4 was synthesized and used in the study of *in vitro* drug accumulation inside leukaemia K562 cell lines. Confocal fluorescence microscopy methods were used to detect the fluorescent signal strength of doxorubicin in the absence and presence of nano Fe_3O_4 . These observations indicated that the tetraheptylammonium-capped nano Fe_3O_4 could efficiently enhance the relevant drug permeation into cancer cells through internalization/endocytosis processes and result in significantly enhanced doxorubicin uptake in respective leukaemia K562 cells [12,13].

In addition to the above mentioned method, a novel electrochemical technique which detects and monitors real-time changes in cell behaviour *in vitro* was used to examine the effects of recognized anticancer drugs on the human ovarian carcinoma cell line and its doxorubicin and cisplatin resistant variants. These cells, adherent to gold electrodes or sensors, modified the extracellular microenvironment at the cell:sensor interface, producing an electrochemical potential that was different from that of the bulk culture medium. Confluent, adherent cells produced an electrochemical signal, measured as an open circuit potential. Exposure of cells to doxorubicin produced positive shifts in the signal compared to untreated control cells during 24 h of cultivation. These positive shifts in signal were evident well before observations of reduced cellular adhesion and viability after 24 h, as judged in parallel cultures with a plastic substratum and by scanning electron microscopy. By contrast, the same treatments applied to the cell lines A2780adr and A2780cispt variants showed that each demonstrated different sensitivities to the same drugs applied to the parental A2780 cells. Although this electrochemical technology readily detects changes in cell adhesion and viability, the modified signals recorded within a few hours of anticancer drug treatments were evident well before microscopic morphological changes become apparent. It can be concluded that these early changes in signals, in comparison to control untreated cells, reflect modifications of physiological/behavioural processes manifested at the cell surface [14].

1.1.2 Monitoring of doxorubicin releasing from nanoparticles

The cross-resistance of certain tumour cells to a series of chemically unrelated drugs is one of the well understood problems in cancer chemotherapy. Multidrug resistance (MDR) can be attributed

to several different biophysical processes including increased drug efflux. This has been found to correlate with the overexpression of the cell surface 170-kDa P-glycoprotein that actively excludes cytotoxic drugs against their concentration gradient. To better understand MDR, experimental methods are needed for studying drug efflux from cancer cells. Continuous measurement of efflux of nonfluorescent drugs on the same cell culture *in situ*, or assessing efflux from a few cells or even a single cell, is beyond the capabilities of existing technologies. A carbon fibre microelectrode was used to monitor efflux of doxorubicin from a monolayer of two cell lines: an auxotrophic mutant of Chinese hamster ovary cells, AUXB1, and its MDR subline, CH(R)C5. Because doxorubicin is both fluorescent and electroactive, the results were validated against existing data obtained optically and with other techniques on the same cell lines, with good agreement found. Based on the results obtained it can be concluded that the electrochemical detection, however, is capable of *in situ* monitoring with high temporal resolution and is suitable for single-cell studies [15]. In addition, Mora et al. showed other type of doxorubicin electrochemical monitoring via an electrochemical protocol for real-time monitoring of drug release kinetics from therapeutic nanoparticles (NPs). The authors used repetitive square-wave voltammetric measurements of the reduction of doxorubicin released from liposomes at a glassy-carbon electrode. It can thus monitor in real time the drug release from NP carriers, including continuous measurements in serum. Such direct and continuous monitoring of the drug release kinetics from therapeutic NPs holds great promise for designing new drug delivery NPs with optimal drug release properties. These NPs can potentially be used to deliver many novel compounds such as marine-life derived drugs and hydrophobic drugs with limited water solubility that are usually difficult to be characterized by traditional analytical tools [16].

It can be concluded that nano-based materials in combination with electrochemistry belong to the promising tools in doxorubicin research. However, there is still lack in the understanding of the basic principles of doxorubicin action. Therefore, the aim of this study was to investigate the interaction of doxorubicin with different sequences of double stranded oligonucleotides (dsODN) using electrochemistry.

2. EXPERIMENTAL PART

2.1 Chemicals

Doxorubicin was purchased from TEVA (Czech Republic). Sodium acetate, acetic acid, water and other chemicals were purchased from Sigma Aldrich (USA) in ACS purity unless noted otherwise. Four types of oligonucleotides and complementary oligonucleotides were from Sigma Aldrich (Table 1). Each of them had ten nucleotides with various sequences of bases. Standard solutions of the oligonucleotide (10 µg/ml) were prepared with ACS water and stored in dark at -20°C. The concentration of oligonucleotide was determined spectrometrically at 260 nm using spectrometer Specord 600 (Analytic Jena, Germany) in quartz cuvettes and thermostat carousel (20 °C). Pipetting was performed by certified pipettes (Eppendorf, Germany).

2.2 Square wave voltammetric measurements

Electrochemical measurements were performed with AUTOLAB PGS30 Analyzer (EcoChemie, Netherlands) connected to VA-Stand 663 (Metrohm, Switzerland) and 797 VA computrace (Metrohm, Switzerland) using a standard cell with three electrodes. A hanging mercury drop electrode (HMDE) with a drop area of 0.4 mm² was employed as the working electrode. An Ag/AgCl/3M KCl electrode served as the reference electrode. Pt electrode was used as the auxiliary electrode. For smoothing and baseline correction the software GPES 4.9 supplied by EcoChemie was employed. Square-wave voltammetric (SWV) measurements were carried out in the presence of acetate buffer pH 5.0. SWV parameters: potential step 5 mV, frequency 280 Hz, time of accumulation 120 s [17]. The analysed samples were deoxygenated prior to measurements by purging with argon (99.999%), saturated with water for 120 s. All experiments were carried out at room temperature (25°C).

Table 1. Four types of double stranded oligonucleotides used in this study.

Name	Sequence	Name	Sequence	Name	Sequence	Name	Sequence
MT5d	5'-CCAAGACAAA 3'-GGTCTGTTT	CA3d	5'-GCTAAAATCC 3'-CGATTTTAGG	GL6d	5'-AATGTTCCAT 3'-TTACAAGGTA	GL4d	5'-TTTTGTAAAC 3'-AAAACATTG

2.3 dsODN preparation

Double-stranded ODNs was prepared by mixing of complementary single-stranded ODNs and then mixture was heated to 99 °C for 15 min under shaking at 400 rpm. Standard solutions of the oligonucleotide concentration 10 µg/ml were prepared and stored in dark at -20°C. The concentration of oligonucleotide was determined spectrophotometrically at 260 nm using spectrometer Specord 600 (Analytic Jena, Germany) in quartz cuvettes and thermostat carousel (20°C).

2.4 Preparation of deionised water and pH measurement

The deionised water was prepared using reverse osmosis equipment Aqual 25 (Czech Republic). The deionised water was further purified by using apparatus MiliQ Direct QUV equipped with the UV lamp. The resistance was 18 MΩ. The pH was measured using pH meter WTW inoLab (Weilheim, Germany).

2.5 Mathematical treatment of data and estimation of detection limits

Mathematical analysis of the data and their graphical interpretation was realized by software Matlab (version 7.11.). Results are expressed as mean ± standard deviation (S.D.) unless noted otherwise (EXCEL®). The detection limits (3 signal/noise, S/N) were calculated according to Long

and Winefordner [18], whereas N was expressed as standard deviation of noise determined in the signal domain unless stated otherwise.

3. RESULTS AND DISCUSSION

Using oscillo-polarography Palecek has already forty years ago discovered that nucleic acids gave two signals: i) redox signal of adenine and cytosine (CA peak), and ii) oxidative signal of guanine [19,20]. Recently elimination voltammetry has been successfully utilized for resolution of reduction signal of adenine and cytosine [21-26]. Moreover it was published that cytosine, adenine, thymine and guanine gave signals at carbon electrodes [27-29]. Based on these promising milestones of electroanalysis of nucleic acids together with the fact that electrochemical methods are still one of the most sensitive analytical techniques, voltammetric methods can be considered as suitable tools for detection of nucleic acids [22,24,30-55].

3.1 Influence of dsODN concentration on CA peak height

dsODN were prepared in renaturation experiment (DNA duplex formation was confirmed spectrometrically). The dependences of CA peak height on concentration of dsODN with the range from 0.5 to 10 $\mu\text{g/ml}$ for all tested oligonucleotide sequences were determined in this study (Fig. 1). Redox signal of adenine and cytosine was observed at potentials around -1.41 (shifting for app 2 mV to a negative potential compared to ssODN) [6]. The concentration dependences had polynomial character with regression coefficient of 0.99 over the concentration range for all analysed dsODN. CA peaks differed according to a specific ODN sequence and their order can be determined by the signal maximum as follows: GL6d < GL4d < MT5d < CA3d. In addition, the studied response of ssODN described in our previous work [6] and dsODN is not identical. Values of potentials are similar for MT5d and GL6d and for GL4d and CA3d (Table 2). However, CA peaks of the lowest concentration of 0.5 $\mu\text{g/ml}$ had the same potentials for all studied dsODNs. The potentials of the peaks grew in the following order with the increasing concentration of ODN: CA3d 98.8 % < MT5d 98.9 % < GL6d 99.6 % < 100 % GL4d (percentages were related to the lowest potential measured in GL4d). Concentration of 0.5 μg oligonucleotide per ml was selected for further measurements, because the concentration is given in the growing part of the calibration curve.

3.2 SW voltammetric analysis of dsODNs interactions with doxorubicin

Typical SW voltammograms of dsODN (0.5 $\mu\text{g/ml}$) measured in the acetate buffer pH 5 (t_A 120 s) are shown in Fig. 2. CA signals were well observed and marked in the voltammograms. However, the changes in the voltammograms were observed after addition of 2.5 $\mu\text{g/ml}$ doxorubicin to the studied dsDNA (90 min., 400 rpm, 25 °C). The decrease in CA peak height and two signals corresponded to doxorubicin called "IC" (-0.4 V) and "OC" (-0.6 V) was observed (Fig. 2). More

details about nature of these signals can be found in the study of Vacek et al. [56]. Intercalation of doxorubicin to double stranded chain in ODN was expected and our results as well as of those of other authors supported this presumption. It is most probable that these results show on strong π - π stacking interaction between nucleic bases and drug [57]. Guanine and adenine are the main targets for the intercalation, whereas much lower interaction occurs with thymine or cytosine (Fig. 3)

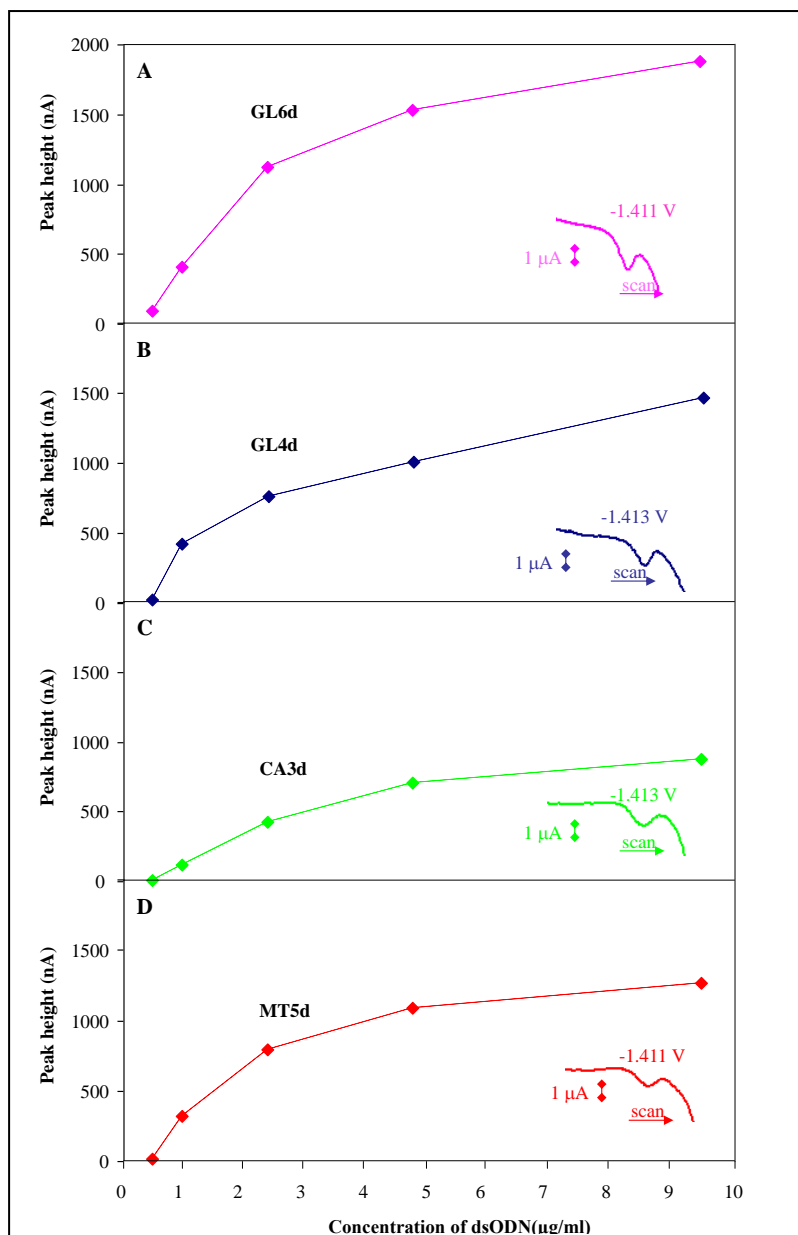


Figure 1. Dependences of dsODN ((A) GL6d, (B) GI4d, (C) CA3d and (D) MT5d) CA peak height on concentration. In the bottom inset in all figures, CA peak is shown. AdTS SW voltammetry: time of accumulation 120 s, potential step 5 mV, frequency 280 Hz. Number of measurement was 10.

Table 2. Potential of CA peak for MT5d, GL6d, GL4d and CA3d (1 $\mu\text{g/ml}$) measured in the presence of acetate buffer pH 5.00. AdTS SW voltammetry: time of accumulation 120 s, potential step 5 mV, frequency 280 Hz. Number of measurement was 10.

CA peak	MT5d	GL6d	GL4d	CA3d
Potential (V)	1.411 ± 0.003	1.411 ± 0.001	1.413 ± 0.002	1.413 ± 0.003

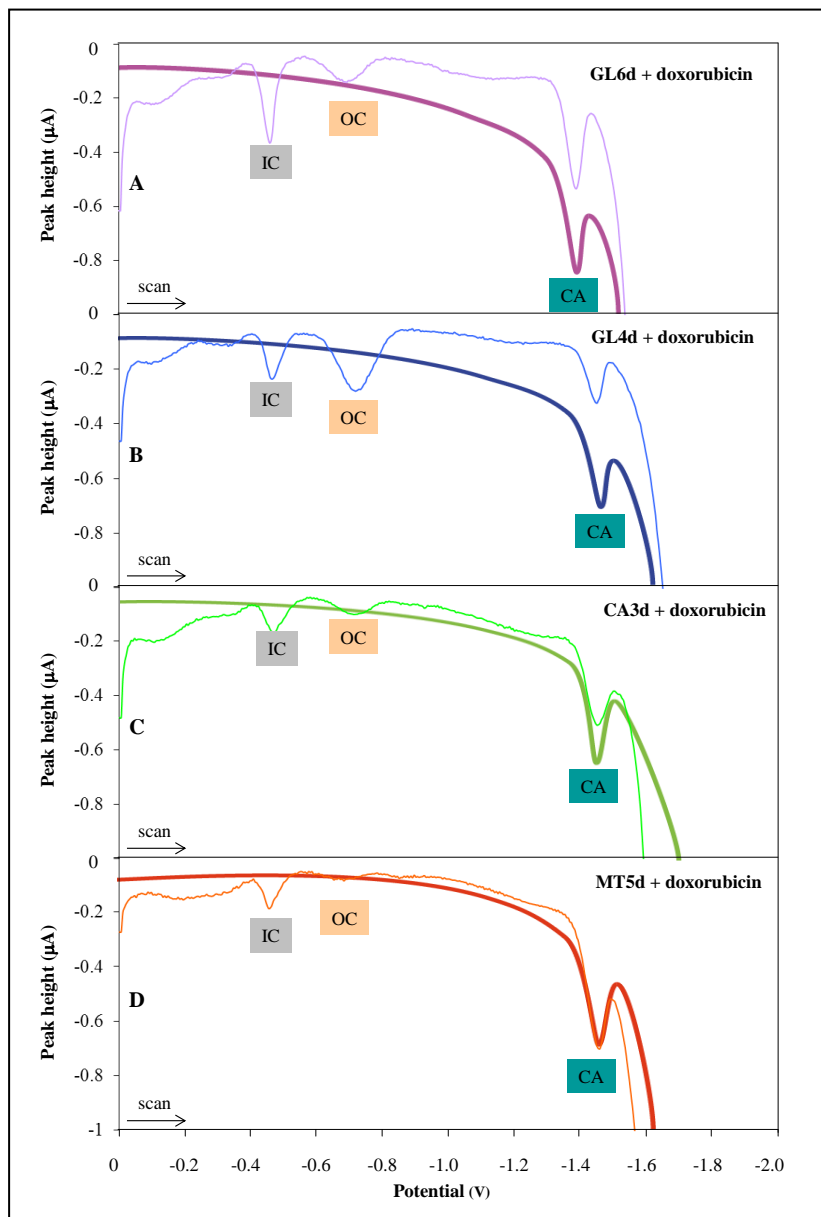


Figure 2. Typical SW voltammograms of (A) GL6d, (B) GL4d, (C) CA3d and (D) MT5d (0.5 $\mu\text{g/ml}$) and its mixture with doxorubicin (2.5 $\mu\text{g/ml}$). Time of interaction 90 min. Light curves correspond to mixtures of oligonucleotide and doxorubicin. Dark curves correspond to pure double-stranded oligonucleotides. Doxorubicin gave two peaks called “IC” and “OC”. For other experimental details, see Fig. 1.

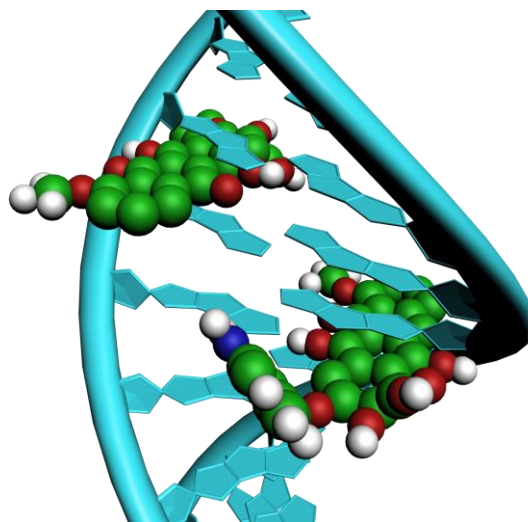


Figure 3. Simple scheme of interaction doxorubicin with dsDNA. Guanine and adenine are the main targets for the doxorubicin intercalation.

In the following experiments, changes of CA and IC peak heights depending on concentration of doxorubicin and time of the interaction (15, 30, 45, 60, 90, 120, 150, 180, 210, 240, 270 and 300 min.) were studied. The CA peak of the studied dsODN (0.5 $\mu\text{g}/\text{ml}$) with no addition of doxorubicin did not change during 300 min. CA peaks measured after 300 min incubation were selected as a reference value (MT5d: 174 nA; CA3d: 100 nA; GL4d: 136 nA; GL6d: 203 nA). The signal is marked by \blacktriangle in Fig. 4. Behaviour of dsODNs was very different from that found for ssODNs [6]. The behaviour of dsODNs was characterized by a decrease in CA from 15 to 60 min incubation, which can be related to intercalation of doxorubicin into dsODN structure. Then the steady-state was reached. The effect of concentration of doxorubicin on CA peak heights of dsODNs was also very interesting. Three ratios of both substances were tested as follows: 1:1, 1:2 and 1:5 (doxorubicin:dsODN). GL6d. The lowest signal of CA was observed in ratio of 1:1 followed by 1:2 and 1:5. There is another interesting phenomenon showing that CA peak of doxorubicin treated dsODNs increased with the increasing time of incubation from 90 min., whereas CA peak measured in a 1:2 ratio reached almost the original CA peak height without any treatment with doxorubicin after 300 min cultivation. This fact can be associated with the interactions of doxorubicin with the outer part of dsODN. This interaction supports marked enhancement of doxorubicin IC peak (Fig. 4A). GL4d curves overlapped for different ratios of oligonucleotide:doxorubicin (dsODN:DOXO). At the time of 15 minutes, the lowest CA peak height was determined in 1:1 ratio followed by 1:2 and 1:5. The CA peak heights decreased with the increasing time of interaction up to 90 min. Further, there was observed steady-state till 150 min. and then slightly increased till the end of the incubation. The values found after 300 min incubation decreased in the following order 1:2 > 1:1 > 1:5 (Fig. 4B). CA3d. At the beginning of measurements, at a time of 15 minutes, the heights of CA peaks were similar for the 1:1 and 1:2 ratios and CA peak of 1:5 was significantly different; it was twice times higher compared to other ratios. These values remained until 60 min., then the peak height of 1:5 ratio decreased rapidly. At the time of 120 min, all curves reached the nearly identical value of the peak height and from this point the peak

heights of all three curves were increasing, while the growth of peaks for ratio of 1:2 was the most intense signal (Fig. 4C). MT5d. The highest decrease in the peak height was observed for 1:5 ratio followed by 1:1 and 1:2 ratios in the first measurement carried out during 15 min incubation.

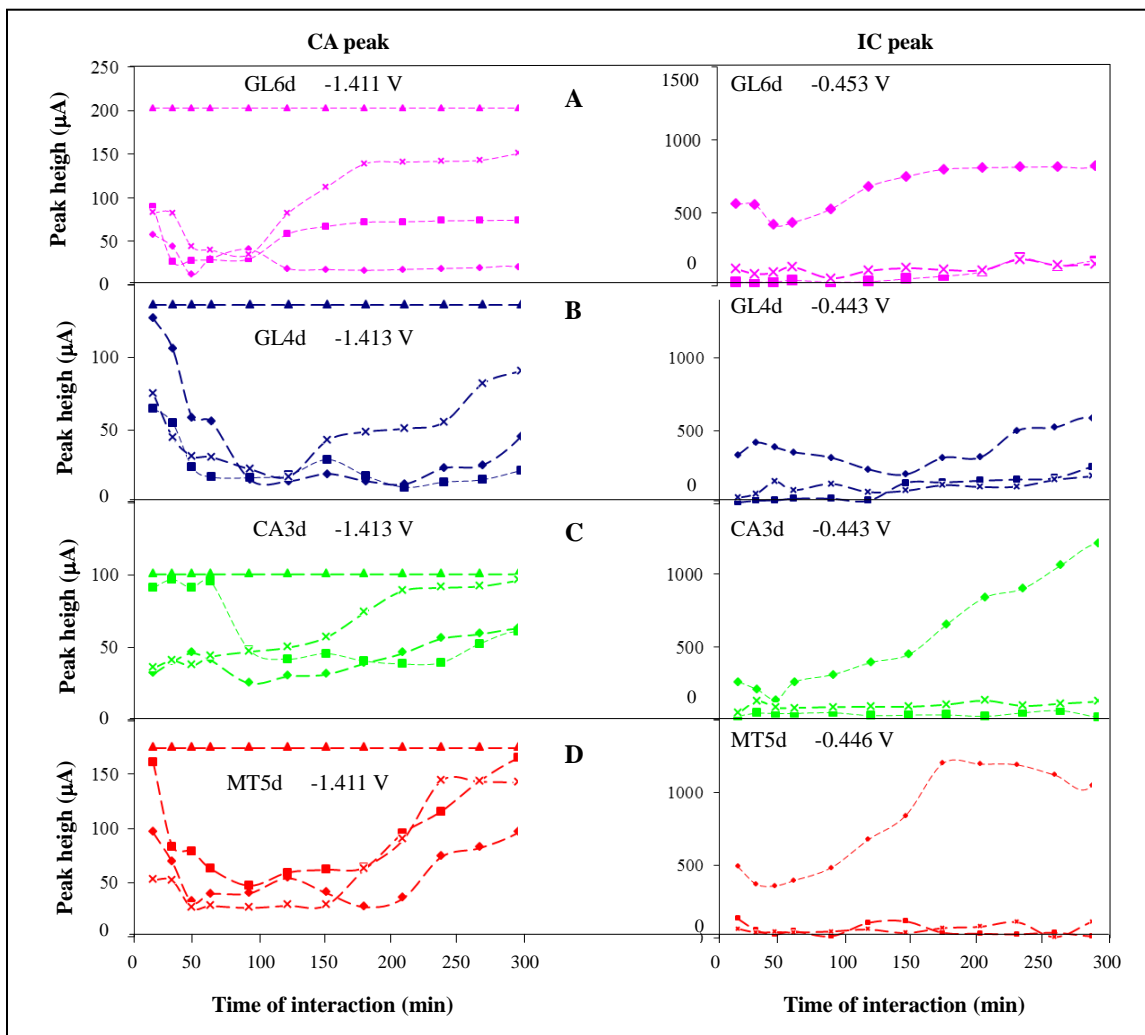


Figure 4. Time of interaction dependence of CA peak height (position -1.41V) and IC peak height (position -0.45V) for the following ratios 1:1(-♦-), 1:2(-x-) and 1:5(-■-) of oligonucleotide:doxorubicin. Reference (-▲-) is average height of CA peaks of studied dsODNs without doxorubicin (n = 10). Interaction was carried out in thermomixer at 400 rpm, 25 °C. For other experimental details, see Fig. 1.

The CA peak heights measured under all tested ratios decreased and did not change until 180 min. After that, a slight increase in the heights was detected. At the end of interaction study, the highest decrease was determined for 1:5 ratio followed by 1:2 and 1:1 (Fig. 4D). We also evaluated the height of the peak signal of doxorubicin called IC at -0.47V. For all dsODNs behaviour of 1:5 (dsODN:DOXO) ratio compared to the others differed markedly. Ratios of 1:1 and 1:2 showed gradual increase in IC peak height. It seems that this signal is associated with doxorubicin intercalation into

dsODN structure. GL4d is at least clear increase in IC peak. Curve ratios of 1:1 and 1:2 have distinct course in GL6d and CA3d (ratio of 1:1 shows a lower signal). The oligonucleotides GL4d and MT5d curves at ratios of 1:1 and 1:2 overlapped (Fig. 4).

CA and IC peaks were correlated in the following part of this study and are summarized in Figs. 5, 6 and 7. Percentage change in the height of CA peak in a mixture of oligonucleotide-doxorubicin was related to the reference value of the height of dsODN peak. Percentage change in peak size DOXO mixed oligonucleotide-doxorubicin was related to the maximum peak value of size in a given time dependence. The obtained data were processed showing the correlation dependence scaling of a IC peak to change the height of each dsODN CA peak. Times of interaction between doxorubicin and dsODN (30, 150, 240 and 300 min.) were inserted to these dependencies. The value of [100, 0] represents the initial state of electrochemical analysis, thus the state of measuring dsODN only. This point must be understood as a starting point for all four of studied oligonucleotides (MT5d, GL6d, GL4d and CA3d).

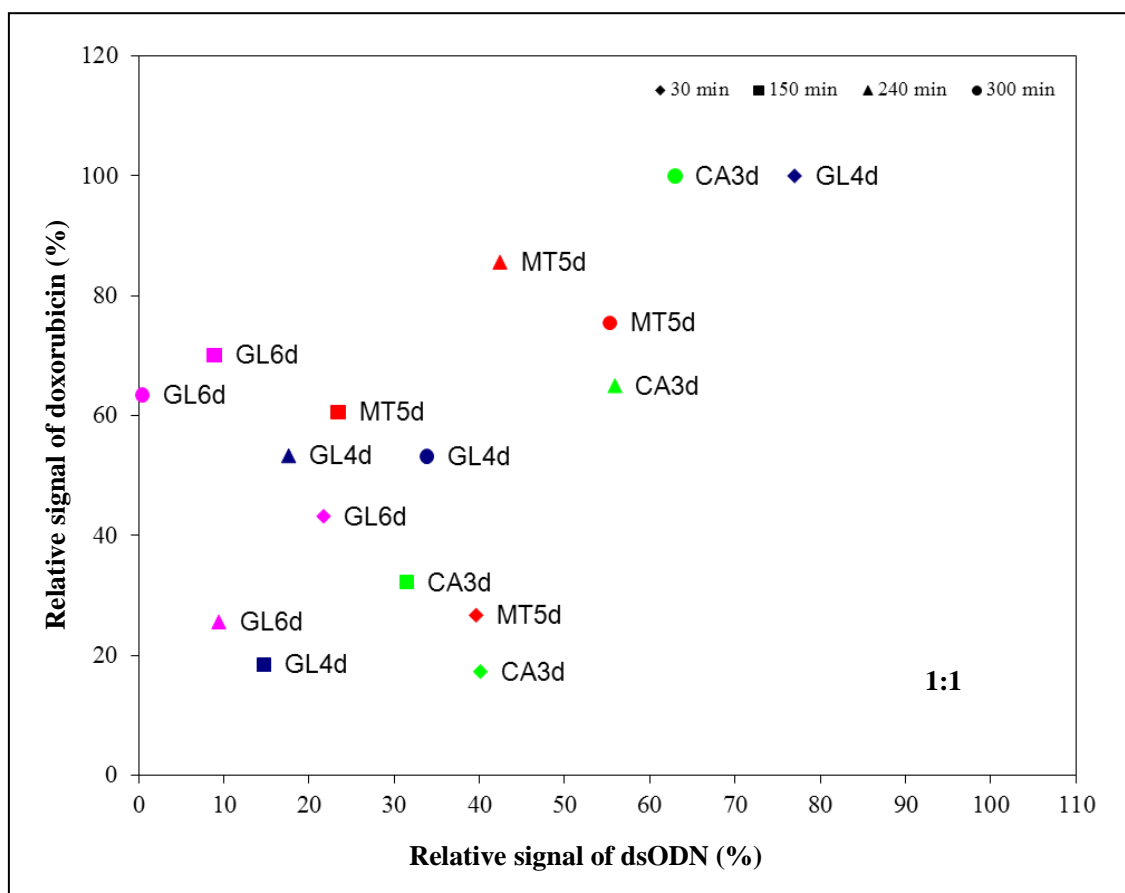


Figure 5. Relative signal of doxorubicin as a function of relative signal of oligonucleotide in ratio 1:1 (oligonucleotide:doxorubicin). Time dependence (30, 150, 240 and 300 min.) for four types of oligonucleotides is presented (MT5d, CA3d, GL4d and GL6d). Relative signal of doxorubicin is relative to maximum value of one time series for each rate. Relative signal of oligonucleotide is relative to average value of signal of pure oligonucleotide. dsODN concentration 0.5 $\mu\text{g/ml}$ and doxorubicin concentration 0.5 $\mu\text{g/ml}$. All experiments were carried out in triplicates. For other experimental details, see Fig. 1.

A mixture of oligonucleotide-doxorubicin mixed in a 1:1 ratio is shown in Fig. 5. A horizontal time sequence for the oligonucleotide CA3d (the lowest values for 30 min, i.e. low doxorubicin content in dsODN at CA peak decline by 60 %) is shown in Fig. 5. With prolonged time, however, the rapid increase in IC peak to CA peak was observed. Very similar results were obtained for MT5d. This shows a significant decrease in CA peak height for more than 80 % compared to control one. With increasing time of the interaction, the peak did not change. It is obvious that GL6d exhibits the most striking changes in electrochemical behaviour. GL6d points are shifted in the diagram to the most left, which indicates a decrease in CA peak height for more than 85 %. Then, there is a dramatic increase in IC peak height, which is related to slight unwinding of dsODN structure. dsODN is then characterized by app. 50% IC peak and by 60-80% decrease in CA peak heights. A very strong interaction was observed in GL6d characterized by the complete disappearance of CA peak. Despite this strong interaction, the maximum IC peak height was within the range from 40 to 80 % (Fig. 5).

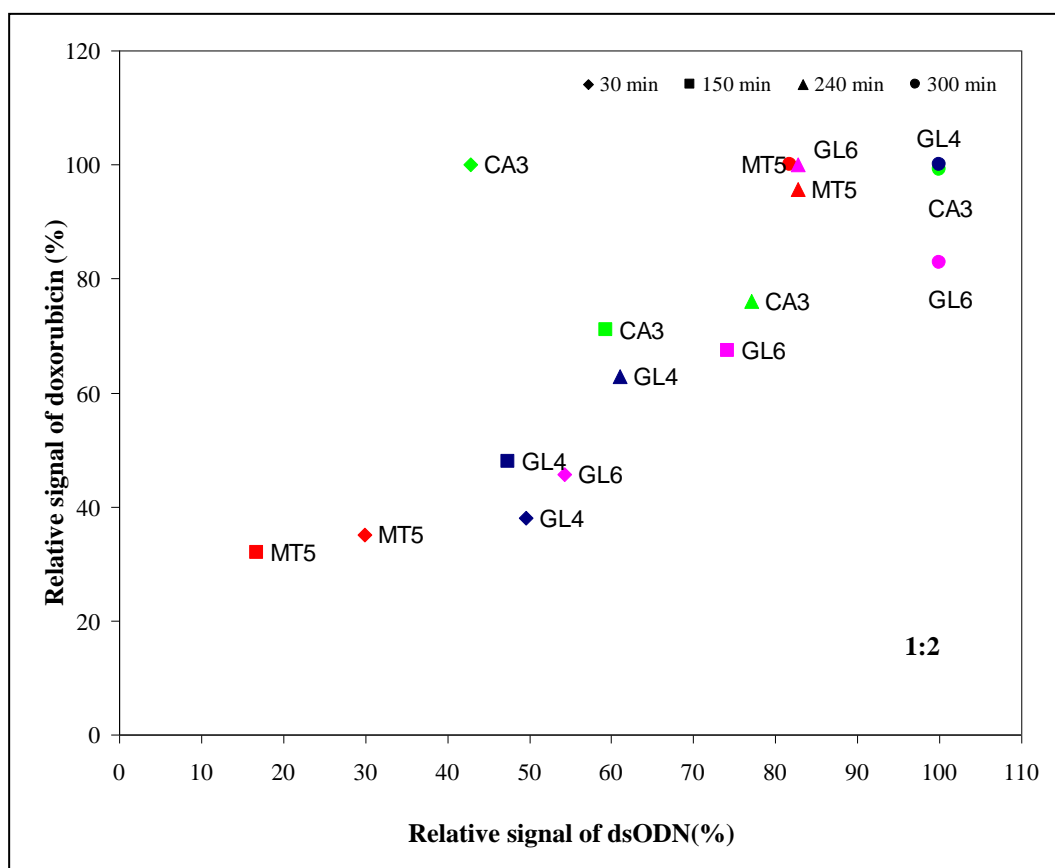


Figure 6. Relative signal of doxorubicin as a function of relative signal of oligonucleotide in ratio 1:2 (oligonucleotide:doxorubicin). Time dependence (30, 150, 240 and 300 min.) for four types of oligonucleotides is presented (MT5d, CA3d, GL4d and GL6d). Relative signal of doxorubicin is relative to maximum value of one time series for each rate. Relative signal of oligonucleotide is relative to average value of signal of pure oligonucleotide. dsODN concentration 0.5 µg/ml and doxorubicin concentration 1 µg/ml. All experiments were carried out in triplicates. For other experimental details, see Fig. 1.

A mixture of oligonucleotide-doxorubicin mixed in a 1:2 ratio provides completely different behaviour in the above-mentioned correlations. There was a marked and significant increase in IC peak accompanied by a decrease in the CA peak. Horizontal timing sequence is shown at GL4d and GL6d. For MT5d, CA peak decreased from 29.9 % measured in 30 min. to 16.8 % measured in 150 min. and then increased to 82.7 % measured in 240 min. and to 81.8% measured in 300 min. (Fig. 6). The course of time dependence for CA3d is interesting. After 30 min., the IC peak was 100% and the CA peak was 42.8%. At the end of the interaction, a CA signal increased up to 100 % and the IC peak height remained unchanged. GL6d, which showed the most significant changes at 1:1 ratio, did not differ from other studied dsODNs. These changes indicate a very complex system of physico-chemical interaction between doxorubicin and DNA (without any biological effect).

A mixture of oligonucleotide-doxorubicin in ratio of 1:5 is shown in Fig. 7. The results obtained show an increase in the IC peak in most of studied dsODNs. It can be noted that there are obvious similarities between GL6d and GL4d.

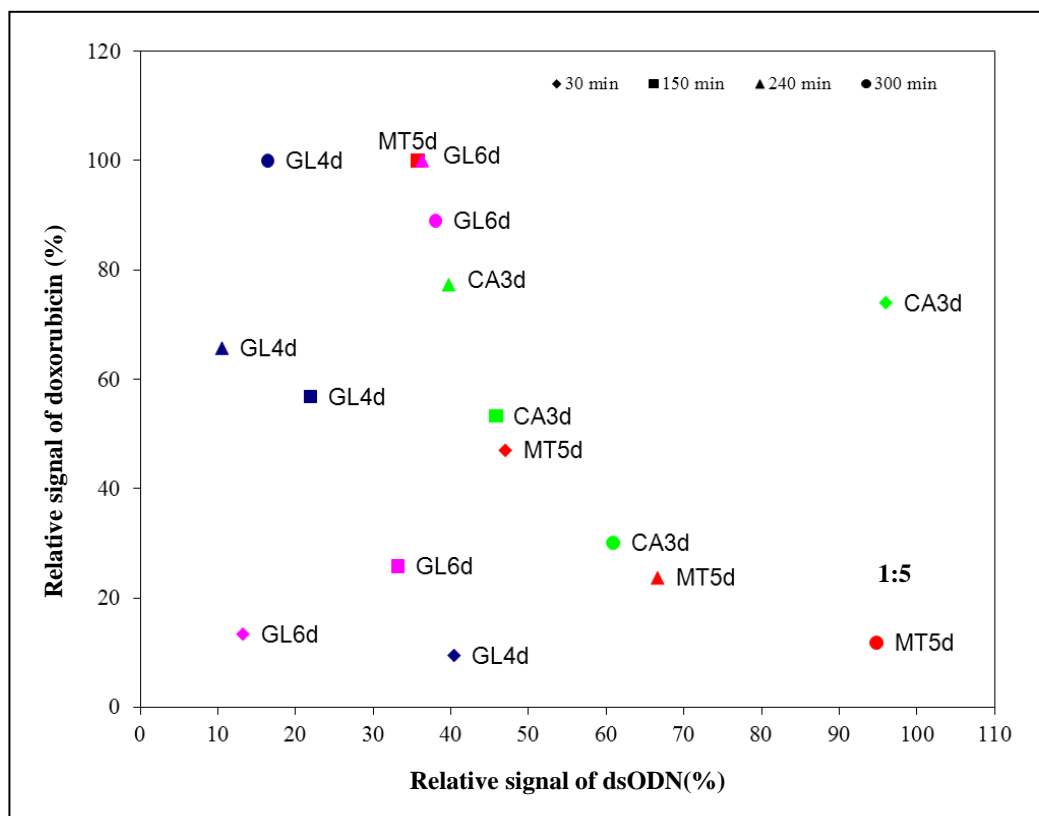


Figure 7. Relative signal of doxorubicin as a function of relative signal of oligonucleotide in ratio 1:5 (oligonucleotide:doxorubicin). Time dependence (30, 150, 240 and 300 min.) for four types of oligonucleotides is presented (MT5d, CA3d, GL4d and GL6d). Relative signal of doxorubicin is relative to maximum value of one time series for each rate. Relative signal of oligonucleotide is relative to average value of signal of pure oligonucleotide. dsODN concentration 0.5 µg/ml and doxorubicin concentration 2.5 µg/ml. All experiments were carried out in triplicates. For other experimental details, see Fig. 1.

The values of the time dependence of both nucleotides are shifted markedly to the left suggesting a significant interaction between doxorubicin and the oligonucleotide (CA peak signal reduction of 60-90% and an increase in the IC peak up to a maximum value). Moreover, apparent horizontal time dependence is observed in both the above mentioned dsODNs. Interactions of CA3d and MT5d with doxorubicin were different; at the end of the interaction study, the IC peak decreased and the CA peak increased, which could be related to structural and conductivity changes (Fig. 7). When comparing the correlation dependencies of the different reaction ratio of 1:1 and 1:2, it seems that the ratio of 1:1 leads to stronger interaction between doxorubicin and oligonucleotides, than at a ratio of 1:2. In the ratio of 1:5 different behaviour of each oligonucleotide was observed. GL4d and GL6d show similarity (strong interaction of both components of the mixture and horizontal time course). Another similarity can be observed in CA3d and MT5d (in 300 min interaction, a decrease in the IC peak and an increase in the CA peak compared to the previous time dependences were detected).

4. CONCLUSIONS

This paper continues on our previous study of Hynek et al. [6]. In the present study we show that the interaction between doxorubicin and dsODN is very complex physico-chemically process. The changes, which can be observed electrochemically, seem to be related to the change in the secondary or other types of structures of studied dsODNs and also probably to the ways of interacting with doxorubicin itself with dsODNs. The type of interaction certainly influences the course of the electrochemical reaction/detection by changing the conductivity of DNA [58,59]. Knowledge of interaction doxorubicin, which is widely used cytostatic drug, with nucleic acids, might be important to rationalize therapy of cancer.

ACKNOWLEDGEMENTS

Financial support from CYTORES GA CR P301/10/0356, NANIMEL GA CR 102/08/1546 and CEITEC CZ.1.05/1.1.00/02.0068 is highly acknowledged. The results were presented at 11th Workshop of Physical Chemists and Electrochemists held in Brno, Czech Republic.

References

1. C. F. Thorn, C. Oshiro, S. Marsh, T. Hernandez-Boussard, H. McLeod, T. E. Klein and R. B. Altman, *Pharmacogenet. Genom.*, 21 (2011) 440.
2. R. Kizek, V. Adam, J. Hrabeta, T. Eckschlager, S. Smutny, J. V. Burda, E. Frei and M. Stiborova, *Pharmacol. Ther.*, 133 (2012) 26. 3. G. Minotti, P. Menna, E. Salvatorelli, G. Cairo and L. Gianni, *Pharmacol. Rev.*, 56 (2004) 185.
4. P. K. Singal and N. Iliskovic, *N. Engl. J. Med.*, 339 (1998) 900.
5. R. R. Patil, S. A. Guhagarkar and P. V. Devarajan, *Crit. Rev. Ther. Drug Carr. Syst.*, 25 (2008) 1.
6. D. Hynek, L. Krejcová, O. Zitka, V. Adam, L. Trnkova, J. Sochor, M. Stiborova, J. Hubalek, T. Eckschlager and R. Kizek, *Int. J. Electrochemical Sci.*, 8 (2012) in press.

7. C. H. Wu, C. Chen and X. M. Wang, Electrochemical contact angle study on biorecognition of doxorubicin with DNA based on the CdS nanoparticles, Southeast Univ Press, Nanjing, 2006.
8. Y. Y. Zhou, L. X. Shi, Q. N. Li, H. Jiang, G. Lv, J. Zhao, C. H. Wu, M. Selke and X. M. Wang, *Biomaterials*, 31 (2010) 4958.
9. J. Y. Li, C. H. Wu, Y. Y. Dai, R. Y. Zhang, X. M. Wang, D. G. Fu and B. A. Chen, *J. Nanosci. Nanotechnol.*, 7 (2007) 435.
10. S. Shen, J. Ren, J. Chen, X. Q. Lu, C. Deng and X. Jiang, *J. Chrom. A*, 1218 (2011) 4619.
11. A. M. Nowicka, A. Kowalczyk, M. Donten, P. Kryszynski and Z. Stojek, *Anal. Chem.*, 81 (2009) 7474.
12. R. Y. Zhang, C. H. Wu, X. M. Wang, Q. Sun, B. A. Chen, X. M. Li, S. Gutmann and G. Lv, *Mater. Sci. Eng. C-Biomimetic Supramol. Syst.*, 29 (2009) 1697.
13. J. Zhou, R. Y. Zhang, X. M. Li, S. Gutmann, G. Lv and X. M. Wang, *J. Nanosci. Nanotechnol.*, 7 (2007) 2942.
14. D. E. Woolley, L. C. Tetlow, D. J. Adlam, D. Gearey, R. D. Eden, T. H. Ward and T. D. Allen, *Exp. Cell Res.*, 273 (2002) 65.
15. C. Yi and M. Gratzl, *Biophys. J.*, 75 (1998) 2255.
16. L. Mora, K. Y. Chumbimuni-Torres, C. Clawson, L. Hernandez, L. F. Zhang and J. Wang, *J. Control. Release*, 140 (2009) 69.
17. D. Huska, V. Adam, P. Babula, J. Hrabeta, M. Stiborova, T. Eckschlager, L. Trnkova and R. Kizek, *Electroanalysis*, 21 (2009) 487.
18. G. L. Long and J. D. Winefordner, *Anal. Chem.*, 55 (1983) A712.
19. E. Palecek, *Nature*, 188 (1960) 656.
20. E. Palecek, *Naturwissenschaften*, 45 (1958) 186.
21. R. Mikelova, L. Trnkova, F. Jelen, V. Adam and R. Kizek, *Electroanalysis*, 19 (2007) 348.
22. L. Trnkova, F. Jelen, J. Petrlova, V. Adam, D. Potesil and R. Kizek, *Sensors*, 5 (2005) 448.
23. L. Trnkova, F. Jelen and I. Postbieglova, *Electroanalysis*, 18 (2006) 662.
24. L. Trnkova, R. Kizek and O. Dracka, *Electroanalysis*, 12 (2000) 905.
25. L. Trnkova, R. Kizek and O. Dracka, *Bioelectrochemistry*, 55 (2002) 131.
26. L. Trnkova, I. Postbieglova and M. Holik, *Bioelectrochemistry*, 63 (2004) 25.
27. V. C. Diclescu, A. M. C. Paquim and A. M. O. Brett, *Sensors*, 5 (2005) 377.
28. A. M. O. Brett and A. M. Chiorcea, *Electrochemistry Communications*, 5 (2003) 178.
29. F. C. Abreu, M. O. F. Goulart and A. M. O. Brett, *Biosensors & Bioelectronics*, 17 (2002) 913.
30. D. F. Colgan and J. L. Manley, *Genes Dev.*, 11 (1997) 2755.
31. J. L. Manley, *Biochim. Biophys. Acta*, 950 (1988) 1.
32. N. J. Proudfoot, A. Furger and M. J. Dye, *Cell*, 108 (2002) 501.
33. D. P. dos Santos, M. F. Bergamini and M. V. B. Zanoni, *Int. J. Electrochem. Sci.*, 5 (2010) 1399.
34. F. Gao, Q. X. Wang, M. X. Zheng, S. X. Li, G. L. Chen and K. Jiao, *Int. J. Electrochem. Sci.*, 6 (2011) 1508.
35. H. Ilkhani, M. R. Ganjali, M. Arvand and P. Norouzi, *Int. J. Electrochem. Sci.*, 5 (2010) 168.
36. R. M. Iost, J. M. Madurro, A. G. Brito-Madurro, I. L. Nantes, L. Caseli and F. N. Crespilho, *Int. J. Electrochem. Sci.*, 6 (2011) 2965.
37. W. Y. Liu and K. J. Zhang, *Int. J. Electrochem. Sci.*, 6 (2011) 1066.
38. H. Y. Shen, X. L. Shao, H. Xu, J. Li and S. D. Pan, *Int. J. Electrochem. Sci.*, 6 (2011) 532.
39. V. Shestivska, V. Adam, J. Prasek, T. Macek, M. Mackova, L. Havel, V. Diopan, J. Zehnalek, J. Hubalek and R. Kizek, *Int. J. Electrochem. Sci.*, 6 (2011) 2869.
40. S. Taufik, N. A. Yusof, T. W. Tee and I. Ramli, *Int. J. Electrochem. Sci.*, 6 (2011) 1880.
41. K. J. Zhang and W. Y. Liu, *Int. J. Electrochem. Sci.*, 6 (2011) 1669.
42. P. A. M. Farias and M. B. R. Bastos, *Int. J. Electrochem. Sci.*, 4 (2009) 458.
43. M. Fojta, L. Havran, R. Kizek and S. Billova, *Talanta*, 56 (2002) 867.
44. R. Kizek, L. Havran, M. Fojta and E. Palecek, *Bioelectrochemistry*, 55 (2002) 119.

45. E. Palecek, S. Billova, L. Havran, R. Kizek, A. Miculkova and F. Jelen, *Talanta*, 56 (2002) 919.
46. E. Palecek, R. Kizek, L. Havran, S. Billova and M. Fojta, *Anal. Chim. Acta*, 469 (2002) 73.
47. M. Fojta, L. Havran, S. Billova, P. Kostecka, M. Masarik and R. Kizek, *Electroanalysis*, 15 (2003) 431.
48. M. Masarik, R. Kizek, K. J. Kramer, S. Billova, M. Brazdova, J. Vacek, M. Bailey, F. Jelen and J. A. Howard, *Anal. Chem.*, 75 (2003) 2663.
49. M. Fojta, L. Havran, R. Kizek, S. Billova and E. Palecek, *Biosens. Bioelectron.*, 20 (2004) 985.
50. E. Palecek, M. Masarik, R. Kizek, D. Kuhlmeier, J. Hassmann and J. Schulein, *Anal. Chem.*, 76 (2004) 5930.
51. L. Trnkova, R. Kizek and J. Vacek, *Bioelectrochemistry*, 63 (2004) 31.
52. S. Krizkova, V. Adam, J. Petrlova, O. Zitka, K. Stejskal, J. Zehnalek, B. Sures, L. Trnkova, M. Beklova and R. Kizek, *Electroanalysis*, 19 (2007) 331.
53. V. Adam, J. Petrlova, D. Potesil, P. Lubal, J. Zehnalek, B. Sures and R. Kizek, *Chem. Listy*, 99 (2005) 353.
54. M. Bartosik and E. Palecek, *Electroanalysis*, 23 (2011) 1311.
55. E. Palecek, *Electroanalysis*, 21 (2009) 239.
56. J. Vacek, L. Havran and M. Fojta, *Electroanalysis*, 21 (2009) 2139.
57. X. Y. Yang, X. Y. Zhang, Z. F. Liu, Y. F. Ma, Y. Huang and Y. Chen, *J. Phys. Chem. C*, 112 (2008) 17554.
58. J. C. Genereux and J. K. Barton, *Nat. Chem.*, 1 (2009) 106.
59. J. D. Slinker, N. B. Muren, S. E. Renfrew and J. K. Barton, *Nat. Chem.*, 3 (2011) 228.